Twinkling Phenomena In Snap-Through Oscillators*

Brian F. Feeny
Department of Mechanical Engineering
Michigan State University
East Lansing, MI 48824–1226

Alejandro R. Diaz
Department of Mechanical Engineering
Michigan State University
East Lansing, MI 48824–1226

Abstract

Oscillatory behavior in a chain of masses connected by springs with continuous but non-monotonic spring forces can be induced under quasi-static loading. Insight into the birth of this behavior is obtained from a single mass system. A bifurcation study shows the potential for equilibrium jumps between multiple equilibria. As such, the transients occurring under quasi-static loading do not converge to the static loading case. Transients during dynamic loading show sensitivity to the loading parameters.

1 Introduction

In this paper we investigate the dynamics of chains of masses connected by springs with non-monotonic spring forces. The work is motivated by the work of Balk, Cherkaev and Slepyan in Refs. [1,2] and in related work in Refs. [3-6]. In Refs. [1,2] the authors use a similar system to explore the dynamics of phase transitions, e.g., in problems where materials can exist in different forms, each characterized by its own energy function. Typically, analysis of these problems is based on Gibbs variational principle, which states that the equilibrium configuration minimizes the total energy in the material mixture. The authors point out in Ref. [1] that this model implies that the system will reach a state of minimal energy in its steady state and observe that the introduction of dynamics changes the problem in unexpected ways. Indeed, using chains of springs with non-monotonic, *discontinuous* spring forces to model the process, the authors show that dynamic effects will actually *prevent* the system from reaching a state of minimum potential energy.

The results in Ref. [1] are of particular interest to us because they suggest a way to design structures capable of dissipating energy at a fast rate. The chain, even when excited quasi-statically, can exhibit high frequency oscillations or *twinkling*. One could take advantage

*Journal of Vibration and Acoustics, 132 (6) no. 061013, 2010

this behavior by transferring energy into these high frequency motions where they will be dissipated more rapidly due to internal friction. In order to explore this idea, we investigate here the behavior of chains of springs with non-monotonic but continuous stiffness, which could be easily manufactured.

This paper is organized as follows. The stability of a *single* degree of freedom system involving springs with non-monotonic but continuous stiffnesses is studied in Section 2. This is followed in by numerical experiments performed on chains of multiple springs to reproduce some of the experiments reported in Ref. [1], this time using continuous stiffness springs. Finally, concluding remarks finish the presentation.

2 Single Degree Of Freedom Pull Test

The work of Balk, Cherkaev and Slepyan in Ref. [1] exhibited an interesting phenomenon. Upon application of a quasi-static displacement at the end of the chain, the equilibrium position of all masses grew quasi-statically. When this equilibrium reached a discontinuity in the spring force, the masses lapsed into a "twinkling" state. In our investigation of the twinkling of systems with springs having continuous non-monotonic spring forces, we first turn to a single degree of freedom. Behavior of the single degree of freedom will provide an explanation for at least some of the behavior that will occur in multi-mass systems. In this section, we look at the local bifurcations of the static equilibria. As such, we will justify the twinkling in terms of bifurcation behavior.

We consider a mass attached to a wall on one side, and to a node (call it P) of prescribed displacement on the other, through nonlinear springs. The qualitative form of the spring force $f(z)$, where z is the deformation in the spring, is shown in Fig. 1. The critical feature of the spring force is its non-monotonicity. On the large scale the stiffness (slope) is positive, but there is an interval in the deformation for which it is negative.

Snap-through and buckled oscillators with a single nonmonotonic elastic member and a directly applied force have also been studied [7-13]. These systems are known to have interesting bifurcations of equilibria, snap-through transients with possibly transient chaos and fractal features, and regular or chaotic steady states. The problem studied here differs by having an imposed node displacement, in contrast to a force applied to a mass, with the mass surrounded by two snap through springs, in contrast to a single grounding spring. As such, this problem has more complicated equilibria and static bifurcations.

2.1 Equilibrium Solutions

The equation of motion for the system is

$$m\ddot{x} + f(x) = f(y - x) \tag{1}$$

where x is the displacement of the mass, and y is the imposed displacement at point P. Then the static equilibrium is given by the solution of

$$f(x) = f(y - x)$$

for x, given y. Figure 2 shows an illustration of this equation. Rather sloppily, we can denote the solution in terms of y as a function of x, as

$$y = x + f^{-1}(f(x)) \tag{2}$$

We use the notation f^{-1} as the *pre-image* of f rather than the inverse, since for some values of x and y, f is not invertible.

In sorting through the equilibrium solutions, it is helpful to look more at the features in Fig. 1. We define the intervals $\mathrm{I_n} = (-\infty, \mathrm{A})$, $\mathrm{I_1} = [\mathrm{A}, \mathrm{B})$, $\mathrm{I_2} = (\mathrm{B}, \mathrm{C})$, $\mathrm{I_3} = (\mathrm{C}, \mathrm{D}]$, and $\mathrm{I_p} = (\mathrm{D}, \infty)$. B and C are in not included in any interval, but this will not pose a threat to our understanding of the equilibria.

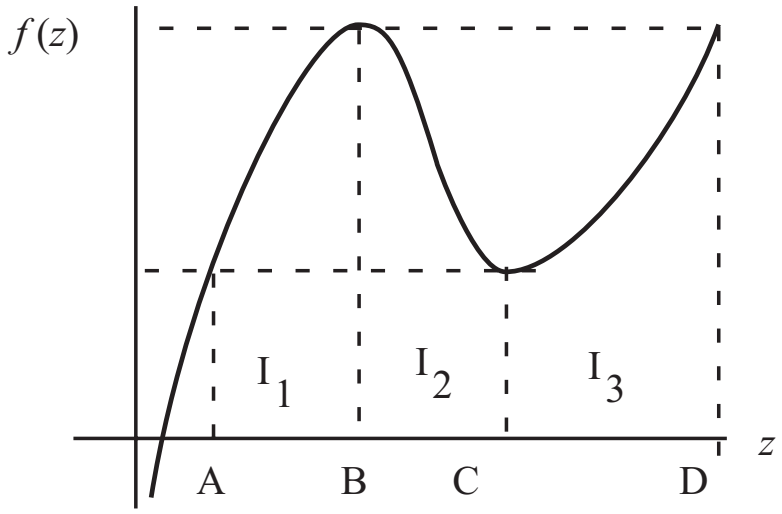

Figure 1: Non-monotonic but continuous force characteristic

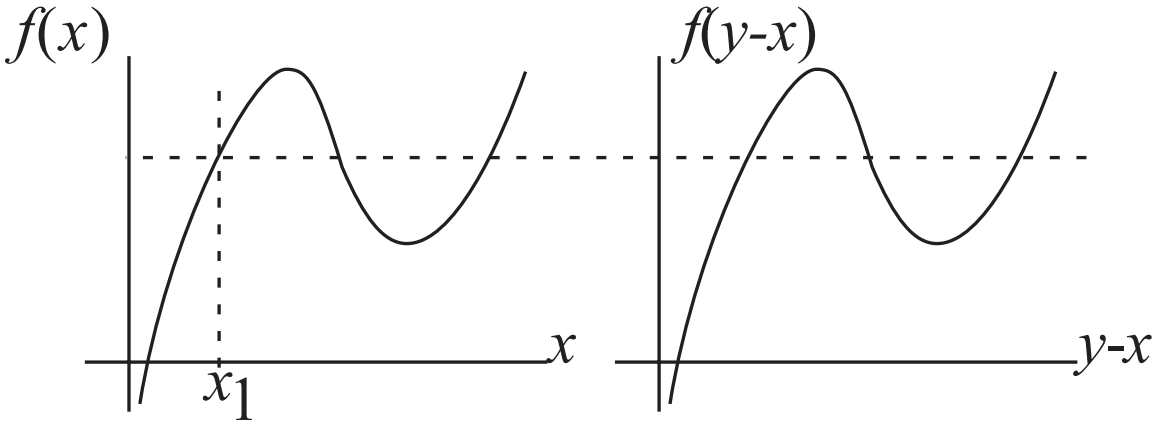

Figure 2: Equilibrium condition that yields multiple equilibrium solutions

In the intervals $\mathrm{I_n}$ and $\mathrm{I_p}$, the function f is indeed invertible. In these intervals, $f^{-1}(f(x)) = x$, and there is a single equilibrium solution at $x = y/2$.

In the noninvertible part of f, we can look at $x + f^{-1}(f(x))$ in terms of the horizontal line in Fig. 2. We define the values x_1, x_2, and x_3 in intervals I_1, I_2, and I_3, respectively, such that $f(x_1) = f(x_2) = f(x_3)$. If x is equal to either x_1, x_2, or x_3, then $f^{-1}(f(x))$ includes x_1, x_2, and x_3. Thus, from (2), for an equilibrium $x = x_1$ in the interval I_1, the possible values of y are $y = 2x_1$, $y = x_1 + x_2$, and $y = x_1 + x_3$. Likewise, for an equilibrium $x = x_2$ in the interval I_2, the possible values of y are $y = x_2 + x_1$, $y = 2x_2$, and $y = x_2 + x_3$. Similarly, for an equilibrium $x = x_3$ in the interval I_3, the possible values of y are $y = x_3 + x_1$, $y = x_3 + x_2$, and $y = 2x_3$.

At values $x = \mathrm{A}$, $x = \mathrm{B}$, $x = \mathrm{C}$, and $x = \mathrm{D}$, there are two possible values of y. For a fixed point at $x = \mathrm{A}$, $y = 2\mathrm{A}$ or $y = \mathrm{A} + \mathrm{C}$. For a fixed point at B , $y = 2\mathrm{B}$ or $y = \mathrm{B} + \mathrm{D}$. For a fixed point at C , $y = 2\mathrm{C}$ or $y = \mathrm{C} + \mathrm{A}$. Finally, for a fixed point at D , $y = 2\mathrm{D}$ or $y = \mathrm{D} + \mathrm{B}$.

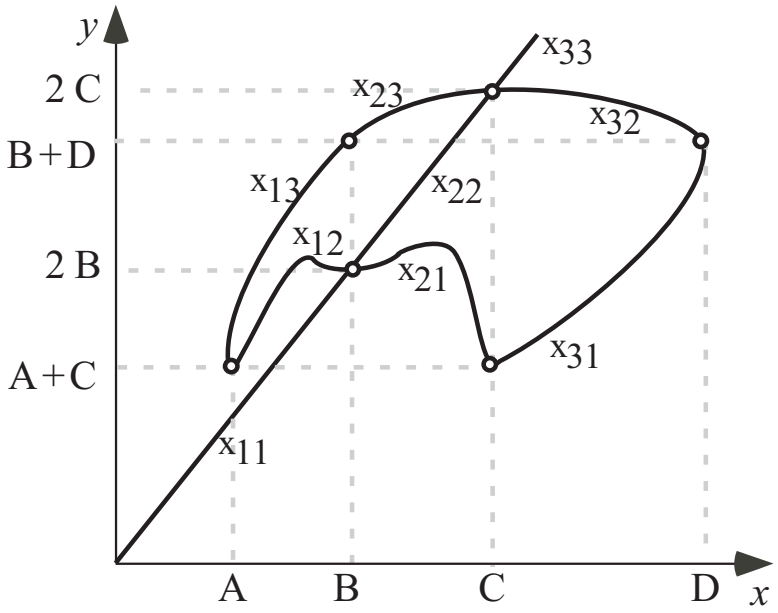

Figure 3: Values of y enabling equilibria of x

Given all of these pieces of information, we can construct a plot of the possible values of y for there to be an equilibrium at x, shown in Fig. 3. The solution branches are labeled according to the discussion in the preceding paragraph, to help distinguish how these solution branches arise. These branch labels are of the form x_{ij} where index i indicates the interval $\mathrm{I_i}$ in which the solution is contained and index j denotes the interval $\mathrm{I_j}$ in which the contributing component of the pre-image $f^{-1}(f(x))$ lies. There is some variation that can occur in this figure. The branches labeled x_{12} and x_{21} are depicted with an undulation, meaning as the solution curve goes from A to B, the x_{12} curve can have a local minimum, an inflection point, and a local maximum, and then merge with the diagonal curve at point B. This undulation may or may not be there, depending on the details of the $f(x)$ curve. The same is true for the x_{21} branch. There is no restriction on whether A+C is less than or greater than 2B, and likewise whether B+D is less than or greater than 2C. These possibilities depend on the $f(x)$ characteristic, and influence the details of the equilibrium curves. We will revisit these

details when we discuss stability.

Inverting this picture provides the plot of fixed points x as a function of parameter y. Depending on the details above, given a value of y, there may be as few as a single equilibrium, or as many as three, five or seven equilibria. Figure 4 shows a couple of cases for the plot of equilibria as functions of y.

A statically forced buckled system has an equilibrium equation $f(x) = F$, producing at most three equilibria for the forms of $f(x)$ considered here. Equilibria curves in Fig. 4 indicate that the two-spring system with imposed displacements is potentially more complicated.

2.2 Local Stability of Equilibria

For an undamped damped single-degree-of-freedom oscillator, local stability is determined by the stiffness term. The system will either be a center (stable) or a saddle (unstable). If we let $x = x_e + u$, where x_e is the equilibrium position, and linearize equation (1) about the equilibrium x_e, the stiffness term has the form

$$f(x_e) + f'(x_e)u - f(y - x_e) + f'(y - x_e)u = [f'(x_e) + f'(y - x_e)]u$$

where $f'(z) = df/dz$. Thus, the linearized equation of motion is

$$m\ddot{u} + [f'(x_e) + f'(y - x_e)]u = 0$$

The equilibrium is unstable if $k = f'(x_e) + f'(y - x_e) < 0$. We can get some qualitative information from Fig. 1. If x_e is in I_1 and $y - x_e$ is in I_1, then clearly $f'(x_e) + f'(y - x_e) > 0$, and the equilibrium is stable. Hence, the solution branch x_{11} in Fig. 3 is stable. If x_e is in I_2 and $y - x_e$ is in I_2, then clearly $f'(x_e) + f'(yx_e) < 0$, and the equilibrium is unstable. Therefore, the branch x_{22} in Fig. 3 is unstable. If x_e is in I_3 and $y - x_e$ is in I_3, then again $f'(x_e) + f'(y - x_e) > 0$, and the equilibrium is stable. Thus, the branch x_{33} in Fig. 3 is stable. Similarly, if x_e is in I_1 and $y - x_e$ is in I_3, or if x_e is in I_3 and $y - x_e$ is in I_1, then $f'(x_e) + f'(y - x_e) > 0$, and the equilibrium is stable. Hence, the branches x_{13} and x_{31} in Fig. 3 are stable. However, if x_e is in I_2 and $y - x_e$ is in I_1 or I_3, or if x_e is in I_1 or I_3 and $y - x_e$ is in I_2, then $f'(x_e)$ and $f'(y - x_e)$ have opposite signs, and more is needed to determine stability. The relative values of the slopes of $f(x)$ and $f(y - x)$ in these cases determine stability. The slopes also are influenced by the relative locations of A, B, C, and D in the $f(x)$ characteristic, which were noted above to influence the details of the equilibrium curves. The function $f(x)$ requires at least cubic terms in its polynomial degree. The cubic term will determine the change in the slopes across the local maximum at B and the local minimum at C .

An analysis of this follows for the case of x_e in I_1 and $y - x_e$ in I_2. In the neighborhood of point $x = \mathrm{B}$, we let $x = \mathrm{B} - \varepsilon u$, where ε is a small bookkeeping parameter, and $y - x = \mathrm{B} + \varepsilon v_1$, where v_1 is then expressed as $v_1 = u + \varepsilon v$. Given εu, εv_1 is determined by the function $f(x)$. We expand $f(x)$ and $f(y - x)$ in Taylor series, noting that $f'(\mathrm{B}) = 0$, yielding

$$f(\mathrm{B} - \varepsilon u) = f(\mathrm{B}) + \varepsilon^2 f''(B)u^2/2 - \varepsilon^3 f'''(\mathrm{B})u^3/6 + \ldots$$

$$f(\mathrm{B} + \varepsilon v_1) = f(\mathrm{B}) + \varepsilon^2 f''(\mathrm{B})v_1^2/2 + \varepsilon^3 f'''(\mathrm{B})v_1^3/6 + \ldots$$

Applying equilibrium, $f(x) = f(y-x)$, allows us to approximate the relationship between u and v_1:

$$\varepsilon^2 f''(\mathrm{B})u^2/2 - \varepsilon^3 f'''(\mathrm{B})u^3/6 = \varepsilon^2 f''(\mathrm{B})v_1^2/2 + \varepsilon^3 f'''(\mathrm{B})v_1^3/6 + \ldots$$

whence, letting $v_1 = u + \varepsilon v$, we have

$$\varepsilon^2 f''(\mathrm{B})u^2/2 - \varepsilon^3 f'''(\mathrm{B})u^3/6 = \varepsilon^2 f''(\mathrm{B})(u+\varepsilon v)^2/2 + \varepsilon^3 f'''(\mathrm{B})(u+\varepsilon v)^3/6 + \ldots$$

Terms of order ε^2 are balanced. Equating terms of order ε^3 leads to

$$v = -f'''(\mathrm{B})u^2/(3f''(\mathrm{B})) = au^2$$

Since the curvature at B is negative, if $f'''(\mathrm{B})$ is positive (likely but not guaranteed, as fine variations in $f(x)$ can take over), then we have $a > 0$. Next, we determine local stability by examining the stiffness term

$$k = f'(x) + f'(y-x) = f'(\mathrm{B} - \varepsilon u) + f'(\mathrm{B} + \varepsilon u + \varepsilon^2 a u^2)$$

Expanding $f'(x)$ and $f'(y-x)$ in Taylor series, and noting $f'(\mathrm{B}) = 0$, we have

$$\begin{aligned} k &= -f''(\mathrm{B})\varepsilon u + f'''(\mathrm{B})\varepsilon^2 u^2/2 + \ldots + f''(\mathrm{B})(\varepsilon u + \varepsilon^2 a u^2) + \\ &\quad f'''(\mathrm{B})(\varepsilon u + \varepsilon^2 a u^2)^2/2 + \ldots = (2/3)f'''(\mathrm{B})\varepsilon^2 u^2 + O(\varepsilon^3) > 0 \end{aligned}$$

for small ε. Thus, on the branch of equilibria labeled x_{12} in Fig. 3, close to the bifurcation point at $x = \mathrm{B}$, the stiffness is positive and the equilibria are locally stable if $f'''(\mathrm{B}) > 0$. We note further that, since $y - x = \mathrm{B} + \varepsilon v_1 = \mathrm{B} + \varepsilon u + \varepsilon^2 a u^2$ and $x = \mathrm{B} - \varepsilon u$, we have $y = x + \mathrm{B} + \varepsilon u + \varepsilon^2 a u^2 = 2\mathrm{B} + a\varepsilon^2 u^2$. This indicates a vertical quadratic tangency in the equilibrium branch for x as a function of y, with positive curvature (unless $f'''(\mathrm{B}) < 0$).

A similar analysis holds for case of x_e in I_2 and $y - x_e$ in I_1. In the neighborhood of point $x = \mathrm{B}$, we let $x = \mathrm{B} + \varepsilon u$, and $y - x = \mathrm{B} - \varepsilon v_1$, where v_1 is then expressed as $v_1 = u + \varepsilon v$. Again, we find that $k = (2/3)f'''(\mathrm{B})\varepsilon^2 \mathrm{u}^2 + O(\varepsilon^3) > 0$, if $f'''(\mathrm{B}) > 0$, for small u. Hence, the branch of equilibria labeled x_{21} is also locally stable if $f'''(\mathrm{B}) > 0$. Again, we find that $y = 2\mathrm{B} + a\varepsilon^2 u^2$ on the branch near the bifurcation point, indicating that the vertical quadratic tangency (if $f'''(\mathrm{B}) > 0$) of x as a function of y holds on both sides of the mother branch. The local bifurcation thus resembles a supercritical pitchfork (subcritical if $f'''(\mathrm{B}) < 0$), Ref. [14].

Similar analysis for the bifurcation at the point $x = \mathrm{C}$ yields similar results for the branches x_{23} and x_{32}. If $f'''(\mathrm{B}) < 0$, the curves local to the bifurcation point bend the opposite direction and are unstable.

Figure 4, plotting x_e as a function of y, shows the stable branches as solid lines, and the unstable branches as dashed lines. The simple equilibria solution, $x_e = y/2$, is stable until x_e reaches $x = \mathrm{B}$ ($y = 2\mathrm{B}$). Then it becomes unstable in what qualitatively matches a supercritical pitchfork bifurcation if $f'''(\mathrm{B}) > 0$ (Fig. 4(b)), and a subcritical bifurcation if $f'''(\mathrm{B}) < 0$ (Fig. 4(a)). Continuing along the $x_e = y/2$ curve, these equilibria become stable,

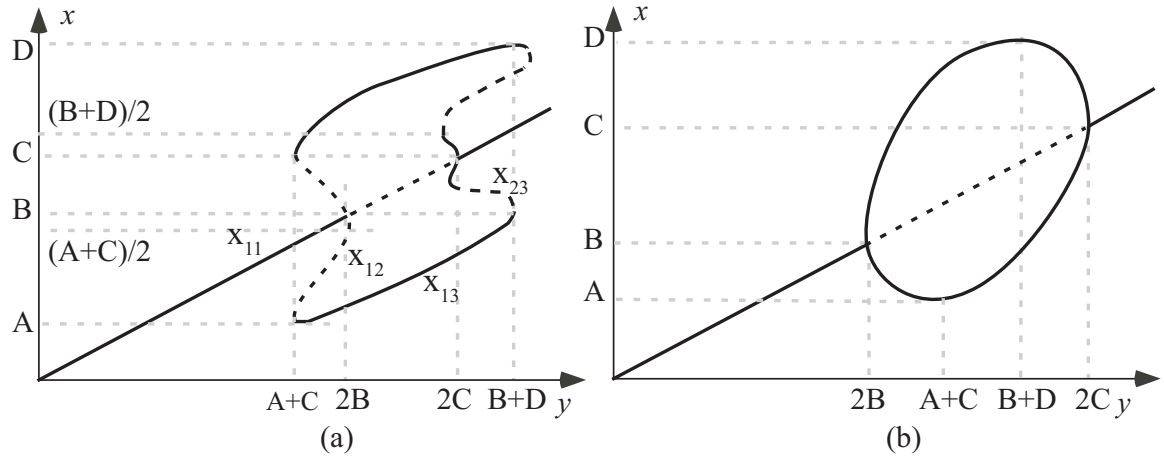

Figure 4: Equilibrium positions in x as functions of imposed extensions y. Solid lines are stable. (a) and (b) are two characteristics, depending on the form of $f(x)$. Part (a) shows examples of branches x_{11} (solid line), x_{12} (dotted), and x_{13} (solid), corresponding to those shown in Figure 3. A branch such as x_{23} contains both stable and unstable intervals (dotted and dashed).

again through a pitchfork bifurcation, at $y = 2\mathrm{C}$. This solution branch remains stable as y increases thereafter.

In the example solution curves of Fig. 4(a), a double saddle-node bifurcation takes place on the branches bifurcating at $x = \mathrm{B}$, and each branch regains stability. In this interval, up to five equilibria are possible for the given y, three of which are stable. In the bifurcation structure shown at $x = \mathrm{C}$, a supercritical bifurcation produces stable branches, which, when followed, pass through a saddle-node bifurcation, losing stability. Further along the branches is another saddle-node bifurcation and regained stability. In this interval, up to seven equilibria are possible for a given y, four of which are stable. In contrast, a mass with a single buckling spring of the same form, and a constant load, could only have as many as three equilibria.

Considering various force characteristics $f(x)$, the curve might have features such as Fig. 4(b). This figure shows at most three equilibria for a given y, with at most two stable equilibria. Two of the saddle-node bifurcations are missing on each off-diagonal branch, in comparison with Fig. 4(a). This figure would be consistent with a $f(x)$ characteristic that was cubic, and of no higher degree. In general, an $f(x)$ characteristic can lead to features seen in either Fig. 4 (a) or (b), in various combinations.

The pitchfork bifurcations are structurally unstable. In a real system, the two nonlinear springs would not be identical. This off symmetry would disrupt the pitchfork bifurcations, replacing them with nearby saddle-node bifurcations. However, the large-scale gist of the set of curves would be preserved for nearly identical nonlinear springs.

2.3 Numerical Examples

If we choose $f(x)$ to be a cubic polynomial, we get an equilibria graph such as Fig. 4(b). Stiffness functions with higher-degree effects lead to more complicated equilibria. Here we show an example of a snap through system with multiple equilibria, by choosing a spring force curve as shown in Figure 5(a). This spring-force function is continuous with a discontinuity in curvature at the inflection point. This produces a set of equilibria, as a function of y, as shown in Fig. 5 (b). The equilibria curves are similar to the branches between $y = \mathrm{A} + \mathrm{C}$ and $y = 2\mathrm{B}$ on Figure 4(a).

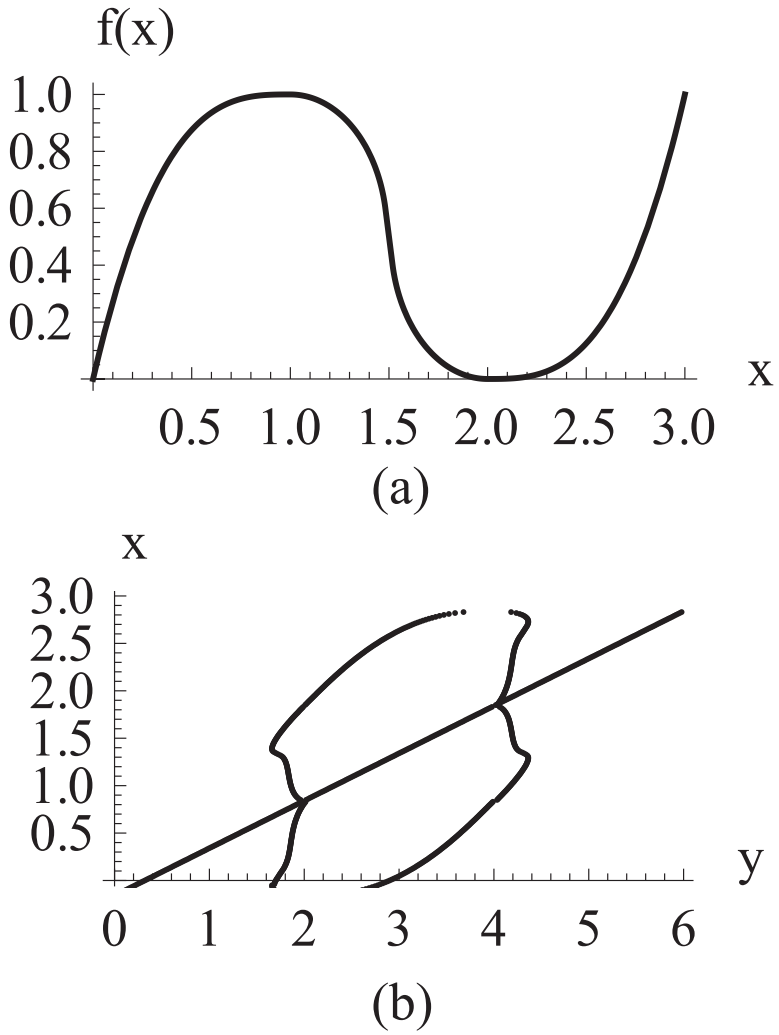

Figure 5: (a) Graph of $f(x)$. (b) Equilibria associated with springs characterized by $f(x)$, as a function of y.

A plot of $f(x) - f(y - x)$ depicts the equilibria as the zeros of the graph for various values of y. For example, if $y = 1$ displacement unit, there is a single equilibrium according to Figure 6(a), which would land on branch of equilibria in Fig. 5(b) corresponding to the branch x_{11} in Figure 4(a), while if $y = 3$, there are three equilibria. The equilibrium with the negative slope at the zero of $f(x) - f(y - x)$ is unstable. As y increases, the middle

equilibrium eventually undergoes a bifurcation, somewhere between the values of $y = 4$ and $y = 4.2$, which are depicted in Figures 6 (c) and (d), as the slope becomes less negative and passes through zero. At this bifurcation, the saddle point stabilizes, and two saddles are produced on either side. The graph of further increased values of y shows these five equilibria, two of which are the new saddles. Finally, if y increases enough, four zeros of $f(x) - f(y - x)$ are lost in two simultaneous saddle-node bifurcations (Fig. 6 (f) is just past the saddle-node bifurcations).

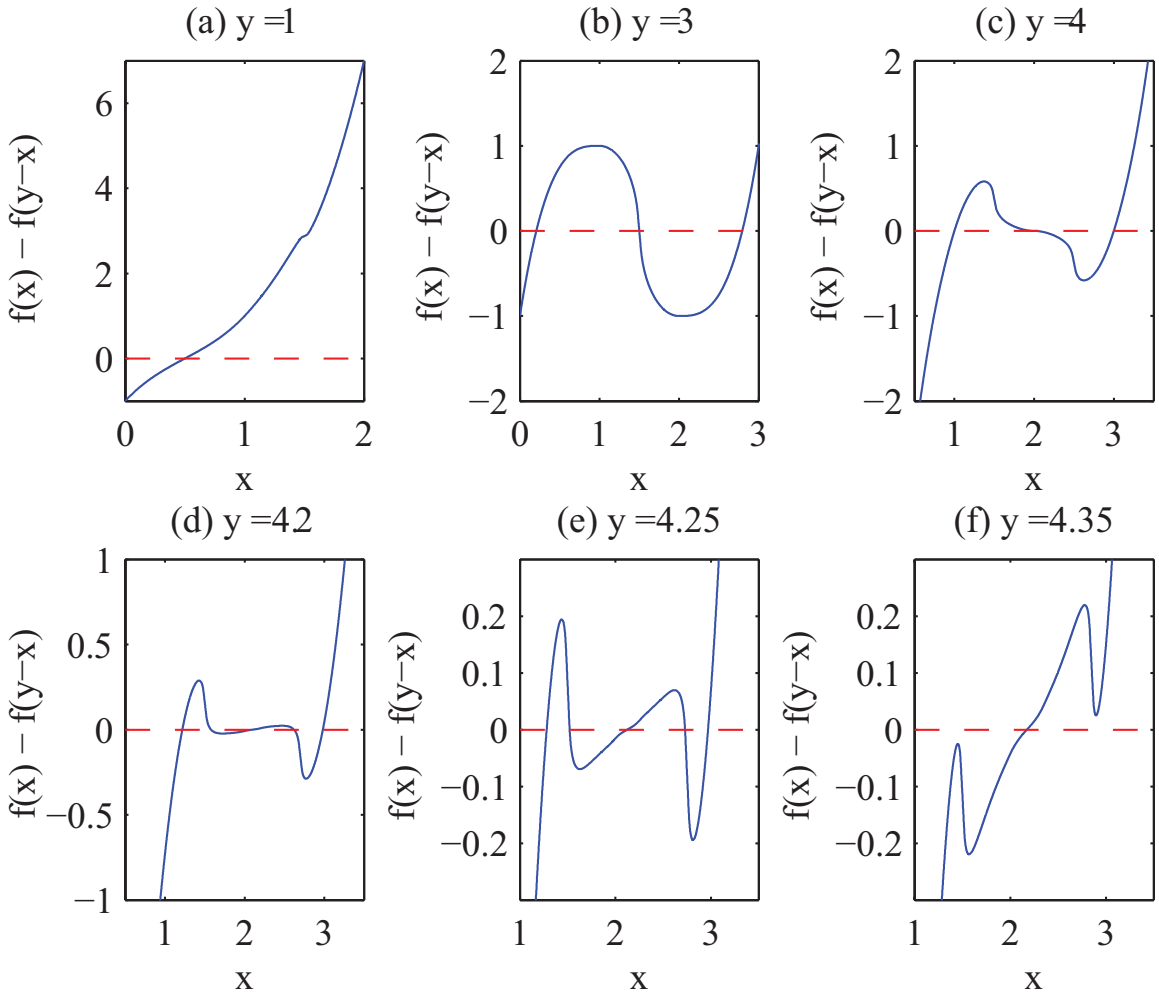

Figure 6: Graphs of $f(x) - f(y - x)$ show zeros which correspond to equilibria, and how they change as y varies. (a) At $y = 1$ there is one zero, (b) at $y = 3$ there are three zeros, (c) at $y = 4$ there are also three zeros, (d) at $y = 4.2$ we see five zeros, (e) $y = 4.25$ has five zeros, and (f) at $y = 4.35$ we see one zero after a double saddle-node bifurcation.

The phase portraits of the undamped system associated with values of y represented in Figure 6 are shown in Fig. 7 (a) – (f). This figure illustrates the multiple equilibria and their stabilities. Neutrally stable center-type equilibria would become stable nodes with the addition of small damping, and correspond to the stable equilibria curves. Saddle equilibria can be inferred in the spaces between sets of periodic orbits associated with the stable

equilibria. Figure 7 (a) has a single center-type equilibrium, while Figure 7 (b) shows two centers and one saddle. In Figure 7(c), the saddle is flattening as it is close to bifurcating, corresponding to the flattening slope in Figure 6(c). After the bifurcation, there are five equilibria, three centers and two saddles, seen in Figures 7 (d) and (e). Figure 7(f) is just beyond the saddle-node bifurcation, in which two pairs of equilibria have merged and vanished, leaving one center. The nearly zero values of the function (Figure 6(e)) cause a set of trajectories to nearly collapse onto the dark circular feature in the plot.

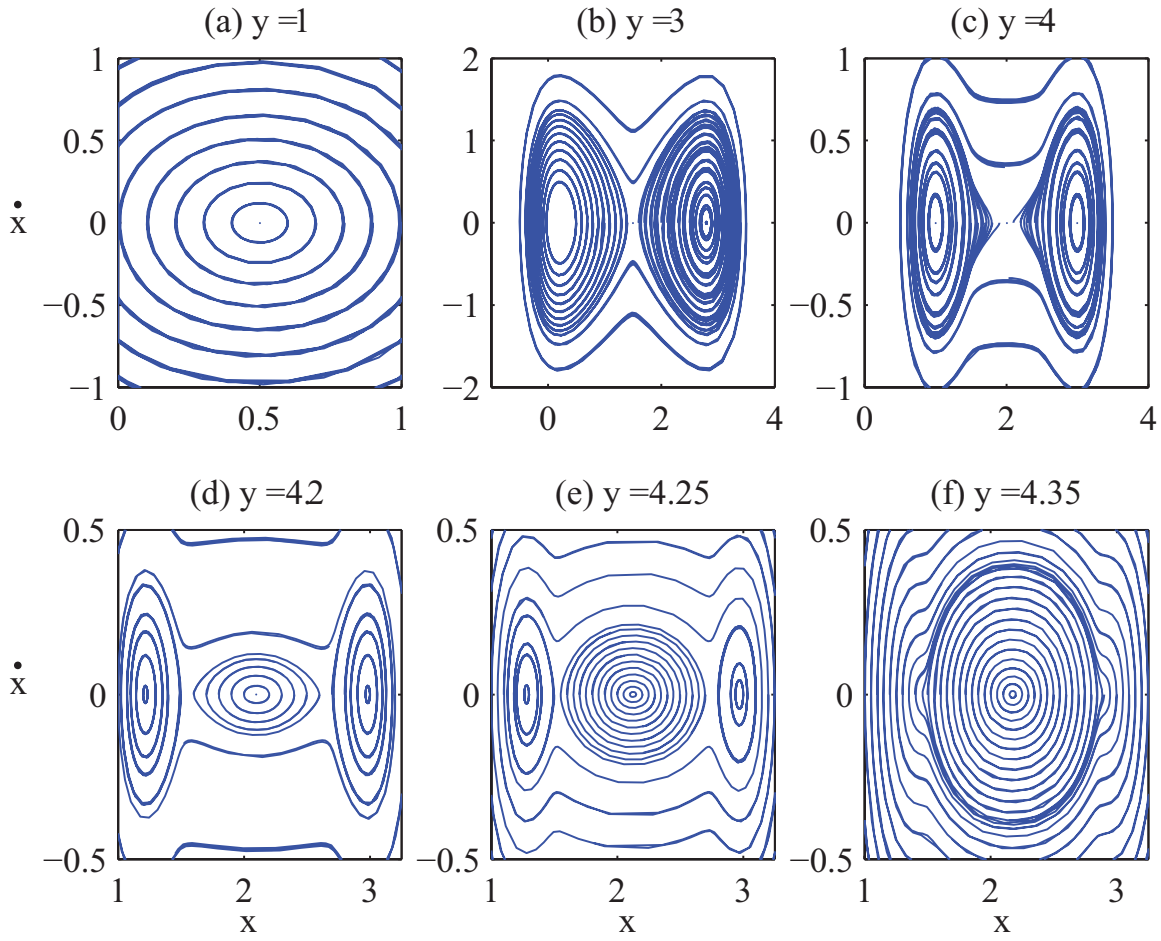

Figure 7: Phase portraits for various values of fixed y illustrate the multiple equilibria, their stabilities, and imply separatrices for the stable equiibria. (a) $y = 1$, (b) $y = 3$, (c) $y = 4$, (d) $y = 4.2$, (e) $y = 4.25$, and (f) $y = 4.35$. Between (a) and (b) there is a pitchfork bifurcation near $y = 2$. Between (c) and (d) there is a pitchfork bifurcation near $y = 4$. Between (e) and (f) there is a pair of saddle-node bifurcations.

2.4 Implications for a Quasi-Static Pull Test

A quasi-static pull test corresponds to a very slow increase (or decrease, for a push test) in y. In our thought experiment, y increases slowly enough that it can be considered constant, suitable for the above analysis of equilibria. Also, while there is no damping in the model,

we consider that a mechanical system will have even a small amount of damping, such that slow changes of equilibria are slower than the decay of transient responses. However, the test is dynamic in the sense that we are interested in transient behavior, should it be significant.

The bifurcation structure for the single degree of freedom provides some indication of the expected behavior of a quasi-static pull test.

Let us first consider a pull test on a system with equilibrium structures similar to Fig. 4(a). If the system is at equilibrium on, for example, branch x_{11}, defined by $y = 2x$, and then y is quasi-statically increased, what happens? When point B is reached, the current solution branch becomes unstable, and the equilibrium solution jumps to either branch x_{21} or x_{23}. Large transient dynamics would then take place before the system settles onto either stable branch. This could be viewed as a twinkling phenomenon. If the system is at equilibrium on, for example, branch x_{33}, defined by $y = 2x$, and then y is quasi-statically decreased to the point C (in a push test for this figure) the branch becomes unstable and there is a continuous, albeit transverse, transition to the equilibrium on the upper and lower branches. Following either branch, it will soon encounter a saddle-node bifurcation, at which the equilibrium vanishes, and the system jumps to another equilibrium, resulting in large transient dynamics before the system settles into a new stable equilibrium, on either branch x_{21} or x_{23}. This, too, could be viewed as a twinkling phenomenon.

If the pull test has finite speed in y, the bifurcation parameter can no longer be considered a constant parameter, and the behavior deviates from the static bifurcation analysis. Detailed transition behavior under slowly varying parameters can be analyzed using singular perturbation techniques, multiple time scales, or the asymptotic methods in Ref. [15-21]. The transverse transition in our problem may be slightly delayed in its onset, and then look sudden, resulting in large transient dynamics before the system settles to a new stable equilibrium, on either branch x_{21} or x_{23}. The particular case of a pitchfork bifurcation is examined in Ref. [21], in which a prediction is made as to which of the new equilibria is approached based on the initial conditions. With very low damping in the model, depending on the rate of the pull, this transient behavior can take the form of an oscillation of significant amplitude. This, too, can be seen as a one-degree-of-freedom twinkling phenomenon, analogous to that observed in Balk, Cherkaev and Slepyan [1].

A similar behavior would be observed in a quasi-static push test through point C.

A quasi-static pull test on a system with equilibrium structure similar to Fig. 4(b) would have slight differences in behavior. When point B is reached, there is a continuous, transverse, transition to the equilibrium on the upper or lower branch. Following either branch would not encounter a saddle-node bifurcation.

In order to encourage twinkling in a quasi-static pull test, the design recommendation is to incorporate a spring with a force $f(x)$ that leads to a picture with either of the features shown in Fig. 4(a). This $f(x)$ would have polynomial contributions of degree higher than three. Such features can be obtained, such that twinkling is encouraged, by pushing the points B and C toward each other. A subcritical bifurcation is expected to induce a larger destabilization jump, and thus larger transients and more "twinkling".

The response of a dynamic pull test would deviate from this discussion on the equilibria curves. However, we conjecture that a dynamic pull test can induce oscillations, or twinkling, if the $f(x)$ characteristic generates a equilibrium structure as in Fig. 4 (a) or (b).

The structural instability can also be exploited in design. Asymmetry in the springs can

be designed to disrupt the pitchfork bifurcation and encourage the quasi-static pull test to follow a chosen curve of Fig. 4 (a), such that the path encounters a maximal jump in the static equilibria upon the saddle-node bifurcation.

2.5 Extension To Higher Degrees Of Freedom

Our analysis approach cannot uncover the details of the equilibria and bifurcation structure for a system with many degrees of freedom. Puglisi and Truskinovsky in Refs. [22-24] were able to categorize the equilibria for small chains by using energy methods, although without the detail of the Section 2.2 on the possibilities for a single mass. For a system with n uniform masses and springs, the diagonal solution $x_j = jy/(n+1)$ exists, and is unstable when the deformation D in the springs are such that the slope in $f(\mathrm{D})$ is negative. This corresponds to the diagonal solution in the single-degree-of-freedom system. It loses stability in a pull test for which the deformation reaches a local extremum in $f(x)$.

To get a feeling for the multi-degree of freedom dynamics associated with the loss of stability we look at numerical simulations.

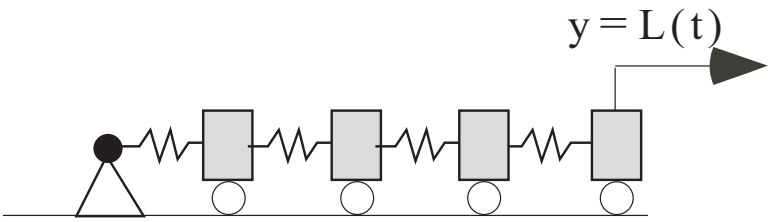

Figure 8: Configuration of 4-mass chain. The motion of the fourth "mass" is imposed.

We investigate the dynamics of the 4-mass chain shown in Fig. 8. Masses at rest are set two distance units apart and then they are connected by springs with the force-displacement function as shown in Fig. 9.

The right mass is given a prescribed displacement $L(t)$ which is increased very slowly until all springs are stretched past the bifurcation point. As in Ref. [1], at the bifurcation point the masses start to oscillate with high frequency, as shown in Fig. 10. This will happen regardless of how slowly the right mass is pulled. This high frequency motion remains even if the system is brought back to its initial configuration ($L = 0$). At that point there is a remnant kinetic energy that is "unrecoverable". This is illustrated in Fig. 11, which shows the total energy as a function of the elongation $L(t)$ for a complete cycle where L is slowly increased to $L = 5$ and then slowly brought back to zero. Finally, a small amount of viscous damping is introduced. As in Ref. [1], this results in a hysteresis in the force-displacement curve of the chain (Fig. 12), again showing that a purely static analysis, e.g., Gibbs variational principle, will not produce the steady state solution of the dynamical system when the excitation itself is quasi-static.

A dynamic pull will also induce oscillations that significantly affect how the masses snap through, depending on the nature of the pull. As an illustration, we included light damping and pulled the end mass as $y = L(t) = vt, 0 < t < 5/v$, and $y = 5$ displacement units for t larger than or equal to $5/v$, letting the masses settle to equilibrium. Figure 13 shows the

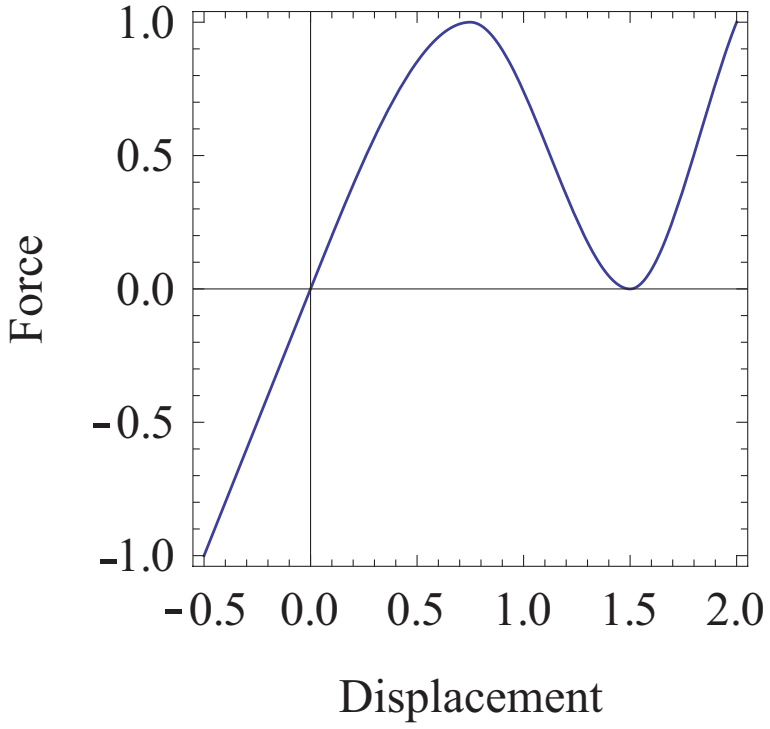

Figure 9: Force-displacement relation for springs in the 4-mass chain

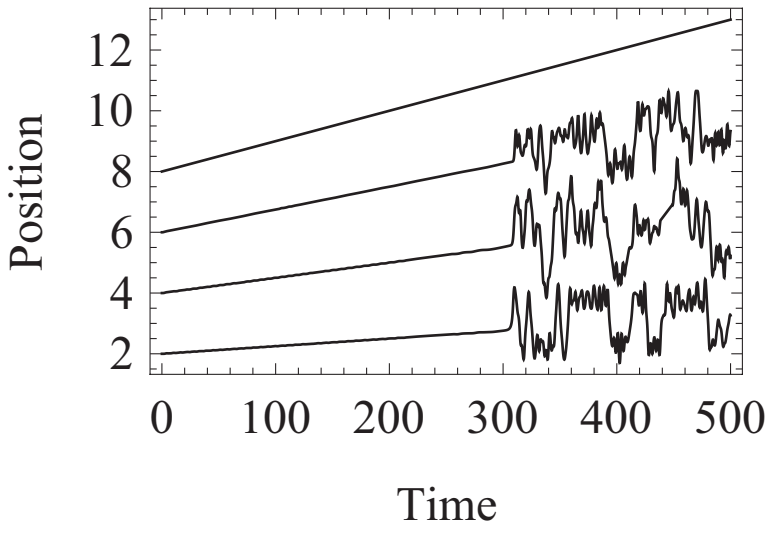

Figure 10: Positions of the 4-mass train when the right mass moves as $L(t)$.

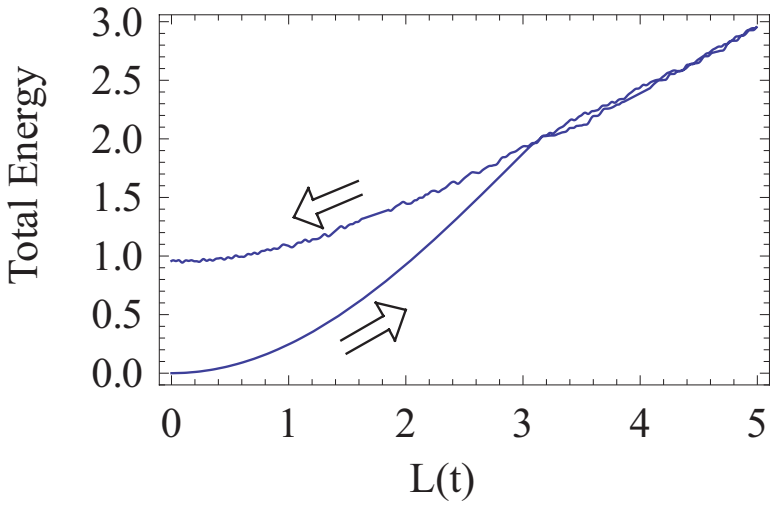

Figure 11: Total energy as a function of total elongation for a full cycle of variation of $L(t)$.

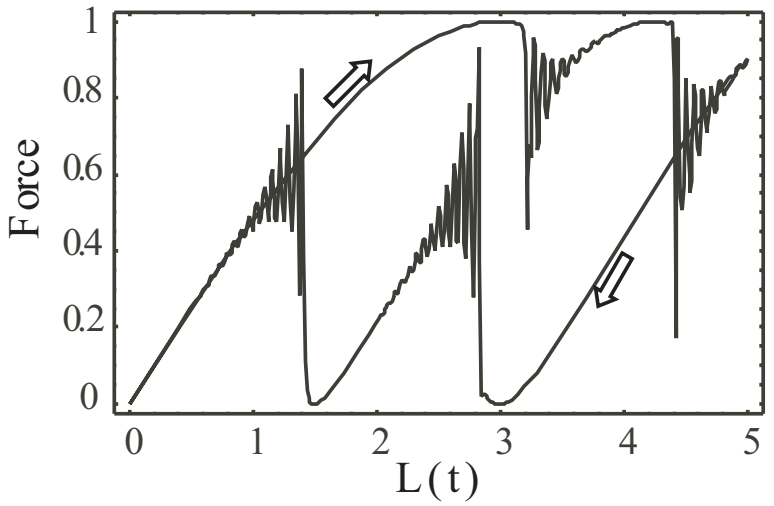

Figure 12: Hysteresis caused by damping for a full cycle of variation of $L(t)$

equilibrium positions reached by each mass for various pulling speeds, v. Masses 1 and 3 can reach four different positions, while mass 2 can reach five positions. The combinations of these mass positions correspond to seven stable equilibria in the six-dimensional phase space with $y = 5$. There are four different possible stable spring lengths for $y = 5$ (Fig. 14). At equilibrium, each spring would have the same force, and there would be two stable snap through configurations for a given force F such that $0 < F < 1$. Thus, with the four possible stable spring *lengths* at equilibrium, there are two possible equilibrium spring *forces*. The intervals in v with large variation of equilibria suggest that there may be fine structure in transient behavior with respect to parameters, and likely also in the basin boundaries in the phase space. Indeed with single-degree-of-freedom buckled oscillators, which have simpler equilibria configurations, basin boundaries can be fractal [13]. This example suggests that the transient dynamics can be very complicated. A larger degree of freedom system is expected be even more complicated.

3 Final Remarks

We have shown that the twinkling phenomenon observed in Ref. [1] for mass chains with non-monotonic discontinuous stiffnesses can occur in chains with smooth, non-monotonic stiffnesses that resemble buckling elements. Under quasi-static loading, the system undergoes a sudden snap through when the springs snap through, inducing high frequency oscillations. A bifurcation study for a single-mass chain provided insight as to how this occurs. The single degree of freedom system undergoes destabilizing bifurcations which may involve jumps in equilibria, depending on the details of the stiffness characteristics. A quasi-static loading does not converge to the static equilibria. Instead, transient oscillations are induced at the bifurcations. These transient dynamics can be very complicated. In future work we will compare the wave propagation through the masses with continuous snap-through elements with that of discontinuous spring elements in Ref. [2].

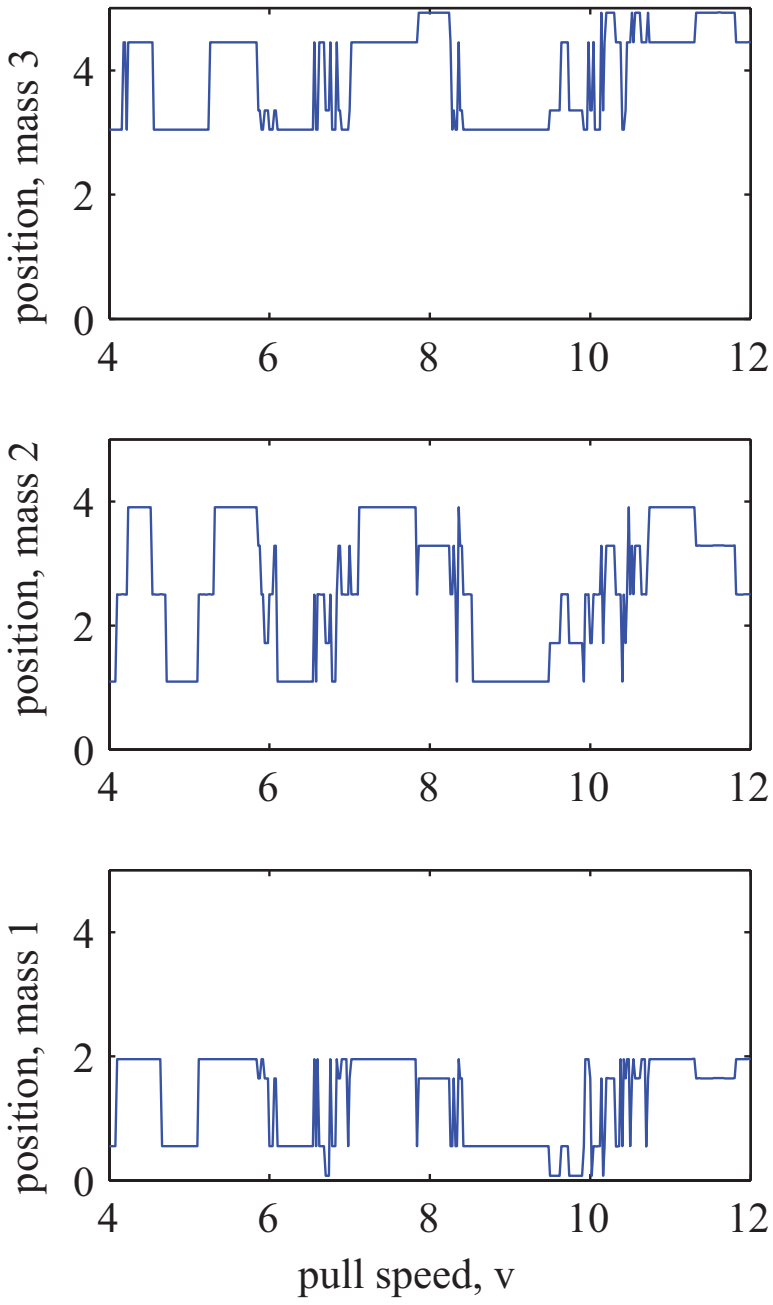

Figure 13: The equilibrium position settled to by each mass when $L = 5$ displacement units is reached at various speeds v.

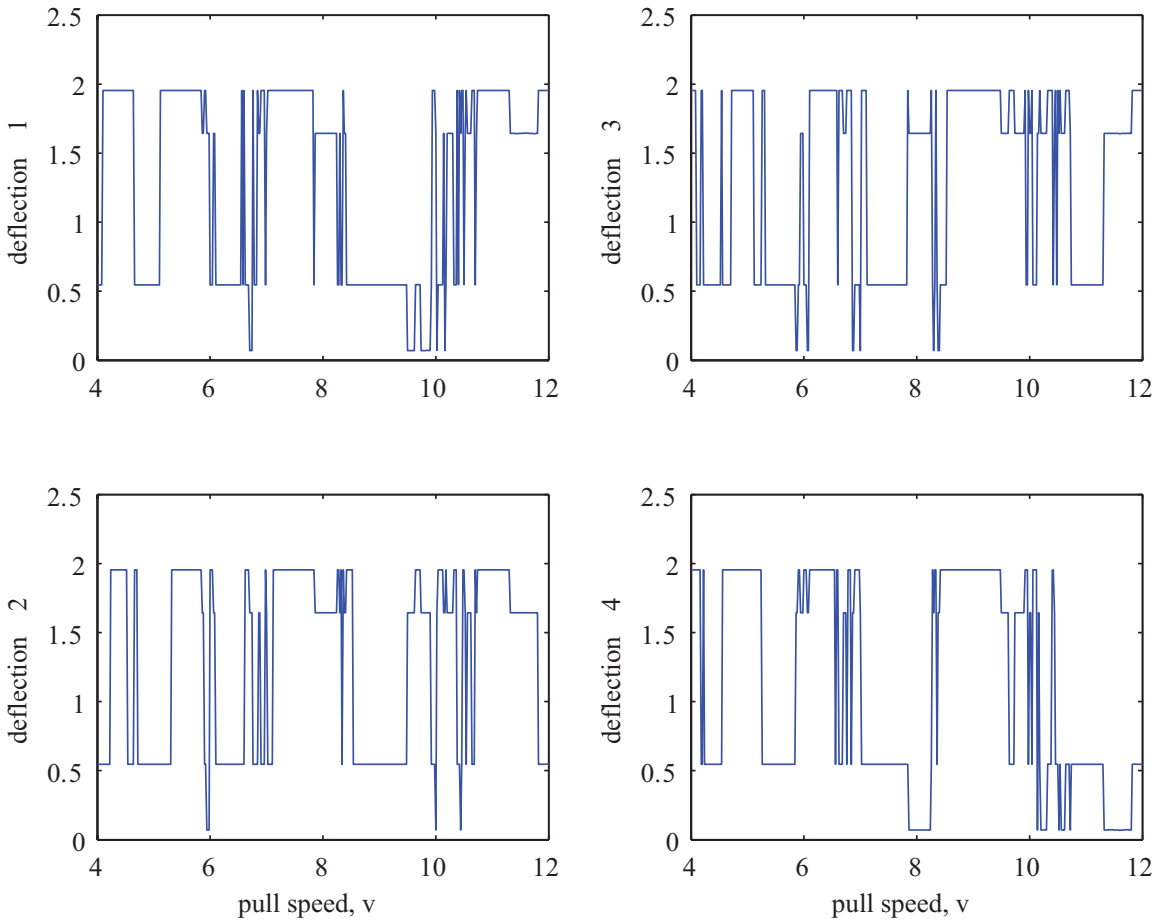

Figure 14: The equilibrium deflection of each spring when $L = 5$ displacement units is reached at various speeds v. For any value of v, the deflections add up to 5 displacement units.

References

[1] Balk, AM; Cherkaev, AV; Slepyan, LI Dynamics of chains with non-monotone stress-strain relations. I. Model and numerical experiments. *J. Mech. Phys. Solids*, 2001; **49** (1):131-148.

[2] Balk, AM; Cherkaev, AV; Slepyan, LI Dynamics of chains with non-monotone stress-strain relations. II. Nonlinear waves and waves of phase transition. *J. Mech. Phys. Solids*, 2001; **49** (1):149-171.

[3] Cherkaev, A; Cherkaev, E; Slepyan, L Transition waves in bistable structures. I. Delocalization of damage. *J. Mech. Phys. Solids*, 2005; **53** (2):383-405.

[4] Slepyan, L; Cherkaev, A; Cherkaev, E Transition waves in bistable structures. II. Analytical solution: wave speed and energy dissipation. *J. Mech. Phys. Solids*, 2005; **53** (2):407-436.

[5] Cherkaev, A; Zhornitskaya, L Protective structures with waiting links and their damage evolution. *Multibody Syst. Dyn.*, 2005; **13** (1):53-67.

[6] Cherkaev, A; Vinogradov, V; Leelavanichkul, S The waves of damage in elastic-plastic lattices with waiting links: Design and simulation. *Mech. Mater.*, 2006; **38** (8-10):748-756.

[7] Gottwald, J. A., Virgin, L. N., and Dowell, E. H., 1995, "Routes to Escape from an Energy Well," *Journal of Sound and Vibration* **187** (1) 133-144.

[8] Johnson, E. R., 1980, "The Effect of Damping on Dynamic Snap-Through," *ASME Journal of Applied Mechanics* **47** (3) 601-606.

[9] Kounadis, A. N., and Raftoyiannis, J., 1990, "Dynamic Stability-Criteria of Nonlinear Elastic Damped Undamped Systems under Step Loading," *AIAA Journal* **28** (7), 1217-1223.

[10] Lock, M. H., 1966, "Snapping of a Shallow Sinusoidal Arch Under a Step Pressure Load," *AIAA Journal* **4** (7) 1249.

[11] Moon, F. C., and Holmes, P. J., 1979, "Magnetoelastic Strange Attractor," *Journal of Sound and Vibration* **65** (2) 275-296.

[12] Holmes, P. J., and Moon, F. C., 1983, "Strange Attractors and Chaos in Non-Linear Mechanics," *ASME Journal of Applied Mechanics* **50** (4B) 1021-1032.

[13] Moon, F. C., and Li, G. X., 1985, "Fractal Basin Boundaries and Homoclinic Orbits for Periodic Motion in a 2-Well Potential," *Physical Review Letters* **55** (14) 1439-1442.

[14] Guckenheimer, J. and Holmes, P. J., 1983, *Nonlinear Oscillations Dynamical Systems and Bifurcation Fields* Springer Verlag, New York.

[15] Haberman, R., 1979, "Slowly Varying Jump and Transition Phenomena Associated with Algebraic Bifurcation Problems," *SIAM Journal of Applied Mathematics* **37**, 69-106.

[16] Lebovitz, N. R., and Schaar, R. J., 1975, "Exchange of Stabilities in Autonomous Systems," *Studies in Applied Mathematics* **54**, 229-260.

[17] Lebovitz, N. R., and Schaar, R. J., 1975, "Exchange of Stabilities in Autonomous Systems–II Vertical Bifurcation," *Studies in Applied Mathematics* **56**, 1-50.

[18] Davies, H. and Krishna, R., 1996, "Nonstationary Response Near Generic Bifurcations", *Nonlinear Dynamics* **10** (3), 235-250.

[19] Raman, A., Bajaj, A.K. and Davies, P., 1996, "On the Slow Transition Across Instabilities in Nonlinear Dissipative Systems," *Journal of Sound and Vibration* **192**(4), 835-865.

[20] Raman, A. and Bajaj, A. K., 1998, "On the Nonstationary Passage through Bifurcations in Resonantly Forced Hamiltonian Oscillators," *International Journal of Nonlinear Mechanics* **33**(5), 907-933.

[21] Maree, G. J. M., 1996, "Slow Passage Through a Pitchfork Bifurcation," SIAM Journal of Applied Mathematics, Vol. 56, No. 3, pp. 889-918.

[22] Puglisi, G; Truskinovsky, L Mechanics of a discrete chain with bi-stable elements. *J. Mech. Phys. Solids*, 2000; **48** (1):1-27.

[23] Puglisi, G; Truskinovsky, L A mechanism of transformational plasticity. *Continuum Mech. Thermodyn.*, 2002; **14** (5):437-457.

[24] Puglisi, G; Truskinovsky, L Rate independent hysteresis in a bi-stable chain. *J. Mech. Phys. Solids*, 2002; **50** (2):165-187.